Journal of Computers Vol. 34 No. 3, June 2023, pp. 335-341
doi: 10.53106/199115992023063403025

Virtual Prototyping Modeling and Fault Diagnosis Technology for Mechanical and Electrical Equipment

Xi-Lin Li[1], Jie Yu[1*], Shi-Ming Zhao[2], Ya-Min Wang[1], Hui-Hua Zhang[1]

[1] School of Automation Engineering, Tangshan Polytechnic College,
Tangshan City 063000, Hebei Province, China
{xilin32987, yujie32543, yamin7788, huihua8795}@163.com

[2] Faculty of Mechanical Engineering, Tangshan Polytechnic College,
Tangshan City 063000, Hebei Province, China
shiming98970@163.com

Received 1 March 2023; Revised 1 April 2023; Accepted 17 May 2023

Abstract. In order to study common faults in motors and motor transmission systems, this article uses a 5kW motor system as an experimental platform to establish a virtual prototype model. The prototype model includes the following five parts: motor unit, 6-degree of freedom loading mechanism, transmission gearbox, loading spindle, and AC excitation converter. Then, the BP neural network is used to identify typical faults in the virtual prototype. The final recognition time for vibration changes, temperature changes, and current disturbances does not exceed 45 seconds, with an average accuracy rate of over 99%. Overall, the algorithm can accurately diagnose typical faults in a relatively short time.

Keywords: virtual prototype, motor fault, BP neural network

1 Introduction

Motors and their transmission systems are widely used in the field of automation, so the daily operation and maintenance of motor systems are particularly important. One of the most frequent faults in the motor system is the misalignment fault in the transmission system. When the transmission system is misaligned, the gears, bearings, couplings, etc. of the gearbox are easily damaged.

Most motor systems are limited by the working environment, making it difficult to collect fault signals. However, virtual prototyping technology can play a sufficient role in simulating motor operation systems and simulating the process of fault generation, so virtual prototyping technology has received attention.

This article mainly focuses on modeling virtual prototypes of typical electromechanical equipment, and then obtains fault feature data through simulation research of the model. Then, artificial intelligence algorithms are used to diagnose faults. Therefore, the work done in this article is summarized as follows:

(1) Established a 5kW motor system as the experimental platform to establish a virtual prototype model;

(2) A BP neural network model for virtual prototype fault diagnosis was established, and the diagnostic results were validated using training and validation sets.

In order to clearly describe the process described in this article, the entire article is divided into the following 6 chapters. Chapter 2 mainly studies the relevant achievements of relevant scholars, providing ideas for this study. Chapter 3 mainly elaborates on the process of establishing a virtual prototype. Chapter 4 uses BP neural network to diagnose typical faults. Chapter 5 is the experimental section to verify the effectiveness of the algorithm. Chapter 6 is the conclusion section, which summarizes the method used in this article, and discussed the next work plan.

2 Related Work

In order to develop a new research method for temperature detectors, Todorov designed a virtual prototype of the

* Corresponding Author

temperature detector and conducted method validation on the virtual prototype [1]. Bushuev described a virtual prototype of a planetary gear hub motor, and based on this, established a joint simulation model of a brushless DC motor control system with PI controller, pulse width modulation (PWM), and Hall effect sensor fault tolerance algorithm. The experimental results were verified using the model [2]. Efstatios designed a data parallel multi gain system prototype framework based on OpenCL for embedded development needs. The framework can achieve rapid restoration and abstract modeling of complex systems [3]. Hengjia Zhu and his team used virtual prototyping technology to improve the calculation method of the rotational inertia of the three wire pendulum rigid body through the law of energy conservation, and established a virtual prototype of the three wire pendulum measurement system, reducing the measurement error by 50% [4]. Jiarui Wang et al. investigated the PVC pulling deformation problem of the clamping stepper device of the blister packaging machine. They established a virtual prototype of the clamping stepper device before and after improvement and conducted dynamic simulation analysis. They compared the motion curves of the stepper device before and after improvement, and obtained an improvement plan through simulation [5]. Xiangpeng Lei used ADAMS software to carry out kinematics simulation for the three grasping configurations of the underactuated manipulator, aiming at the problems of imperfect characteristics and limited load of the three manipulators. The optimization results effectively enhanced the structural performance and load capacity of the manipulator [6].

3 Virtual Prototype Modeling

The main faults of the motor and transmission system are mainly concentrated in the transmission part. Therefore, a model of the motor system is established and load analysis is conducted to judge the faults based on the analysis results. This article uses a 5kW motor system as an experimental platform to establish a virtual prototype model, which includes the following 5 parts: motor unit, 6-degree of freedom loading mechanism, transmission gearbox, loading spindle, and AC excitation converter.

3.1 Modeling of the Transmission Part

The 6-degree of freedom loading mechanism controls the force of 6 hydraulic cylinders through a computer, providing loads in 5 directions other than torque. The 6 load directions are shown in Fig. 1.

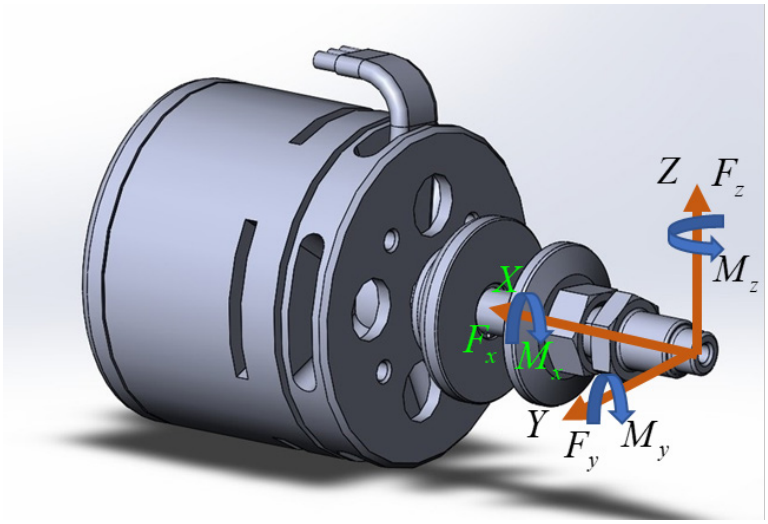

Fig. 1. Virtual prototype of electric motor

The key to the virtual prototype simulation model of the motor unit lies in the design and research of a 6-degree of freedom loading mechanism. The loading mechanism applies the load to the dynamic platform through six servo hydraulic cylinders, which are then transmitted to the hub of the loading spindle. One end of the hydraulic pressure is connected to the platform, the other end of the hydraulic cylinder is connected to the dynamic platform, and the dynamic platform is fixedly connected to the loading spindle. Based on the motor power of 5kW and the maximum load at the spindle hub where the motor system is loaded, the design selects the motor, reducer, loading spindle, and coupling. SolidWorks software is used to establish a test platform part model for the motor unit, and the established part model is imported into Adams software. Constraints between each part are applied in Adams software to establish a virtual prototype model of the test platform, as shown in Fig. 2.

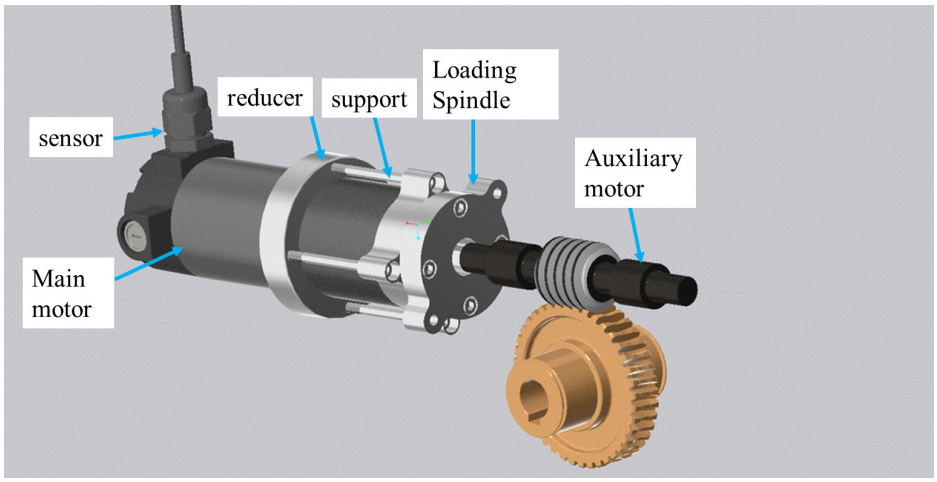

Fig. 2. Transmission system structure

The 6-degree of freedom loading mechanism consists of a hydraulic cylinder body, a hydraulic cylinder piston rod, a bracket, and a loading plate. There are degrees of freedom between the cylinder body and the bracket, as well as between the loading plate and the hydraulic cylinder piston rod [7].

The transmission gearbox is a two-stage planetary gear, and its transmission route is as follows: 1) Low speed stage: main transmission shaft → planetary carrier → planetary gear → sun gear → 2) Medium speed stage: planetary carrier → planetary gear → sun gear → 3) High speed stage: driving large gear → driven small gear, motor output shaft and reducer input shaft are connected by fixed pairs, and reducer output shaft and universal coupling are connected by fixed pairs. A universal coupling is a component consisting of four components, connected by two universal pairs and one prism pair. The interior of the transmission gear is shown in Fig. 3.

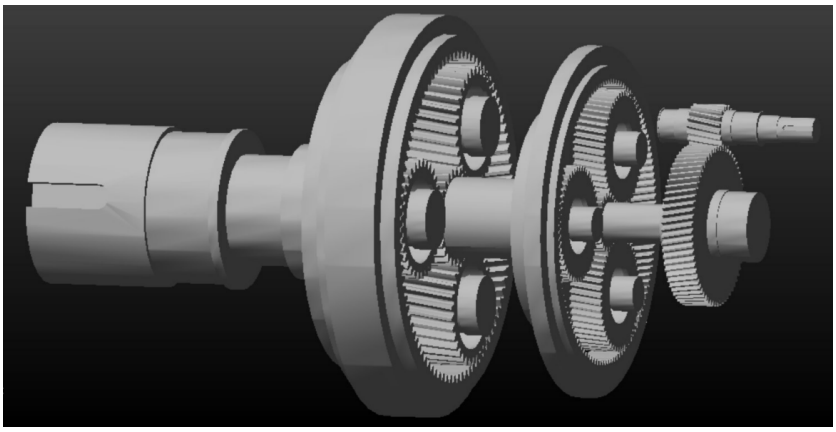

Fig. 3. Internal structure of transmission gear

The universal joint coupling of the loading mechanism of the virtual prototype transmits the torque and motion of the motor to the loading spindle, which is connected with the loading spindle by a fixed pair in two weeks. The 6-DOF loading mechanism applies the remaining 5 DOF loads to the hub of the loading spindle by hydraulic drive.

3.2 Modeling and Simulation of AC Excitation Converter

The AC excitation converter used in the motor is a dual PWM converter [8], which can be used as a rectifier or inverter. This part needs to achieve variable speed constant frequency operation of the motor group while decoupling and controlling the active and reactive power output of the stator. Let the stator flux ψ_s on the d-axis and q-axis components be:

$$\frac{d\psi_{ds}}{dt}=0,\frac{d\psi_{qs}}{dt}=0. \tag{1}$$

In order to achieve variable speed and constant frequency operation of the electric unit, the electronic voltage U_s can be controlled appropriately by directing U_s on the d-axis to obtain:

$$\begin{cases} u_{ds}=U_s \\ u_{qs}=0 \end{cases}. \tag{2}$$

The equations of active power P_s and reactive power Q_s, as well as the stator flux equation, can be obtained as follows:

$$\begin{cases} P_s=\dfrac{3}{2}u_{ds}i_s \\ Q_s=-\dfrac{3}{2}u_{ds}i_{ds} \end{cases}. \tag{3}$$

$$\begin{cases} i_{ds}=-\dfrac{L_m}{L_s}i_{ds} \\ i_{qs}=-\dfrac{L_m}{L_s}i_{qr}-\dfrac{U_s}{L_s\omega_1} \end{cases}. \tag{4}$$

In the formula, i_{ds} and i_{dr} are the stator current and rotor current in the d-axis direction, i_{qr} and i_{qs} are the rotor and stator current in the q-axis direction, respectively. The stator output Ps is controlled by controlling i_{dr} and i_{ds}, and the stator output Q_s is controlled by controlling i_{qr} and i_{qs}.

After controlling U_s appropriately, the output electromagnetic torque T_e of the generator is expressed as:

$$T_e=1.5n_p\frac{L_m}{L_s}\frac{U_s}{\omega_1}i_{dr}=1.5n_p\frac{L_m}{L_s}\psi_s i_{dr}. \tag{5}$$

In the formula, L_m is mutual inductance, L_s is phase inductance, and the T_e of the generator is proportional to i_{dr}. When i_{dr} changes, T_e changes proportionally, and the rotor speed changes accordingly.

4 Improved Algorithm for Motor Group Fault Diagnosis

This article uses BP neural network to diagnose misalignment faults in motor units. The faults caused by misalignment are nonlinear classification faults. In the process of dealing with linear fault classification, BP neural

network has more advantages [9].

Assuming that the neural network has L hidden layer and n neural nodes, each of which has a *Sigmoid* function excitation. The activation function of neurons between the hidden layer and the output layer is $f(x)$ and $g(x)$, respectively. Given the input and output $(x_k, y_k)(k = 1, 2, 3, ..., N)$, given that the j unit of the l layer inputs the k sample, the input of node j is:

$$net_{jk}^{l} = \sum_{j} w_{ij}^{l} H_{jk}^{l}. \tag{6}$$

Where, w_{ij}^{l} represents the connection weight coefficient of the input layer and the middle hidden layer, H_{ij}^{l} represents the output of the j -th neuron node when the input of the layer $l-1$ neural network is in the k sample, and error function represents E represents:

$$E_k = \frac{1}{2}\sum_{j}(y_{lk} - \bar{y}_{lk})^2. \tag{7}$$

$$E = \frac{1}{2N}\sum_{k=1}^{N} E_k. \tag{8}$$

In the formula, y_{lk} is the output when the k -th sample is input to layer l , E_k is the output error when the k -th sample is input, and E is the total output error of the neural network. In the process of neural network training, compare the error function with the preset accuracy for judgment. If the accuracy requirements are not met, correct the weight to reduce the error until the accuracy meets the requirements or the number of iterations reaches the upper limit.

5 Improved Algorithm for Motor Group Fault Diagnosis

For the diagnosis of motor axis misalignment faults, 10 neurons are established in the BP neural network, and 4 neurons are established in the output layer. The adaptive learning rate is added to the beam factor gradient descent backpropagation algorithm for training. The maximum allowable training steps are set to 500 steps, the learning rate is 0.01, and the minimum error of the training target is 0.01. The traingdm function is used as the training function, and the error transformation of the training results is shown in Fig. 6, The horizontal axis in the figure represents the number of iterations and the vertical axis represents the mean square deviation. As shown in the figure, after 41 iterations, the error accuracy meets the requirements, and the training results are shown in Fig. 4.

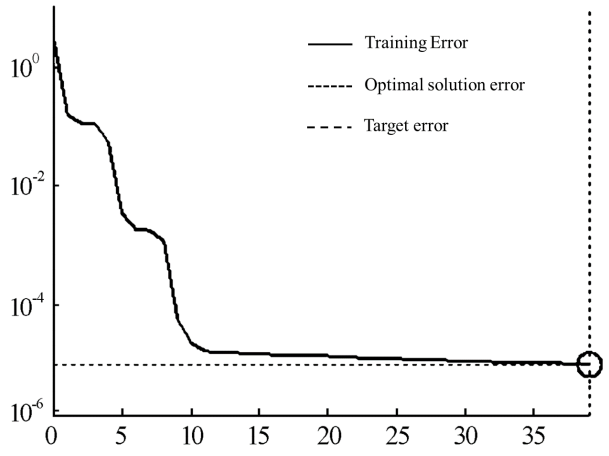

Fig. 4. Change in training error

Using BP neural network to run 38 tests, the diagnostic results include running time, training set classification accuracy, and test set classification accuracy. The running results of the trained BP neural network are shown in Fig. 5, which are explained in terms of running time and recognition accuracy. In order to facilitate analysis, a neural feedforward network (RBF) is introduced for comparison.

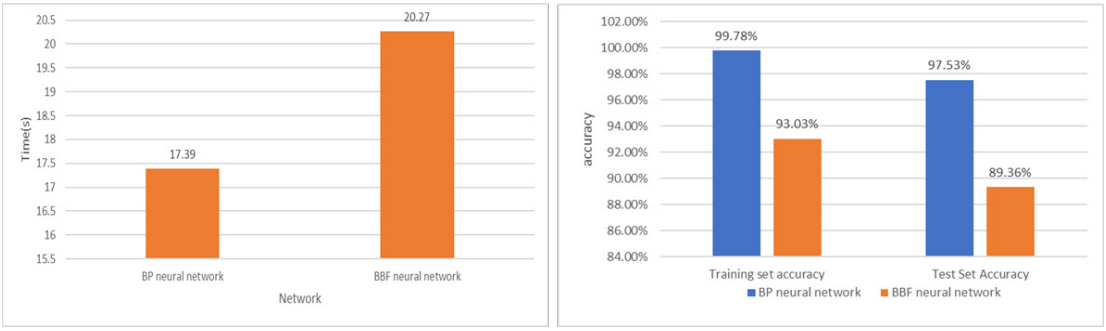

Fig. 5. Run time and Accuracy comparison

In order to demonstrate the superiority of the method described in this article, the typical disturbances caused by motor misalignment, such as vibration, temperature changes, and stator current, are identified and diagnosed, and corresponding diagnostic results are obtained the result is shown in Fig. 6.

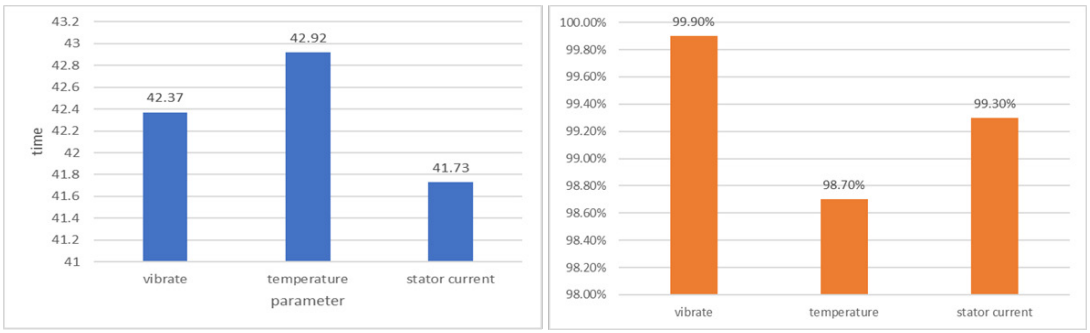

Fig. 6. Comparison of fault diagnosis time

As shown in the figure, the method proposed in this article has a good recognition effect on vibration changes, temperature changes, and current disturbances caused by misalignment of the motor unit. The operating time does not exceed 45 seconds and meets the requirements. For the training set, the average classification accuracy exceeds 99%, with a high accuracy rate. For the test set, the classification accuracy can also reach 99%. Overall, the algorithm can accurately diagnose typical faults in a relatively short time.

6 Conclusion

In order to study common faults in motors and motor transmission systems, this paper uses a 5kw motor system as an experimental platform to establish a virtual prototype model. Then, a BP neural network is established for virtual prototype fault diagnosis model, and the diagnosis results are verified using training and validation sets. Then, the BP neural network is used to identify typical faults in the virtual prototype. The final recognition time for vibration changes, temperature changes, and current disturbances does not exceed 45 seconds, with an average accuracy rate of over 99%. Overall, the algorithm can accurately diagnose typical faults in a relatively short

time.

There are still some shortcomings in this article, which are also the direction of future research. I will be committed to more in-depth research.

(1) The established motor model is slightly simpler, while today's motor transmission systems are more refined and complex;

(2) The established model has a single category and should further establish more diverse motor models and application scenarios, which can diagnose more diverse situations.

7 Acknowledgement

Exploration and practice of improving curriculum ideological and political ability of electromechanical teachers in higher vocational colleges (TSSKL2023-156).

References

[1] G. Todorov, K. Kamberov, T. Ivanov, Parametric optimisation of resistance temperature detector design using validated virtual prototyping approach, Case Studies in Thermal Engineering 28(2021) 101302.

[2] D.A. Bushuev, T.Y. Kiseleva, V.G. Rubanov, Virtual prototype for co-simulation of hub-motor dynamics with brushless DC motor and elements of fault-tolerant control, IOP Conference Series: Materials Science and Engineering 560(1) (2019) 012103.

[3] E. Sotiriou-Xanthopoulos, L. Masing, S. Xydis, K. Siozios, J. Becker, D. Soudris, OpenCL-based Virtual Prototyping and Simulation of Many-Accelerator Architectures, ACM Transactions on Embedded Computing Systems (TECS) 17(5)(2018) 1-27.

[4] H.-J. Zhu, C.-Y. Kuang, X. Lv, A Calculation Method and Virtual Verification For the Rotational Inertia Considering the Cycloid Mass Effects of the Trifilar Pendulum, Machine Tool & Hydraulics 50(19)(2022) 109-114.

[5] J.-R. Wang, D.-Q. Zhang, Y. Li, Analysis Improvement and Dynamic Modeling of Stepping Device Based on Virtual Prototype, Journal of Liaoning University of Technology (Natural Science Edition) 41(6)(2021) 373-378.

[6] X.-P. Lei, Y.-F. Liu, Virtual Design and Parameter Optimization of Under-actuated Three-Finger Manipulator Based on ADAMS, Computer Measurement & Control 28(11)(2020).

[7] Y.-S. Wang, X.-H. Zeng, H.-Y. Chen, X.-J. Li, G.-H. Li, Modeling and Control of Motor of Power-split Hybrid System, Science Technology and Engineering 20(12)(2020) 4968-4976.

[8] X.-M. Wang, H. Cheng, L. He, J.-F. Wu, Research on modeling and control technology of six-phase induction motor with double Y-connected 3-phase symmetrical windings displaced in turn by 30°, Ship Science and Technology 42(15) (2020) 140-144.

[9] D.-H. Li, L.-H. Xu, D.-Y. Long, X. Wang, T. Qin, J. Yang, Photovoltaic Array Fault Diagnosis with Genetic Algorithm Optimized BP Neural Network, Microprocessors 42(6)(2021) 23-26.